660 *Chem. Mater.* **1991**, *3*, 660–667

peak atomic ratios of peak $1_{N(1s)}$/total C(1s) and peak $1_{Si(2p)}$/total C(1s) increases at powers ≥20 W, indicating an overall increase of Si_xN_y to SiC at the surface because peak 1 in both the N(1s) and Si(2p) envelopes corresponds to Si_xN_y species.

The formation of an overlayer Si_xN_y with increase in microwave power is also reflected in Table VIII, which summarizes the atomic ratios of the component peaks of the O(1s), Si(2p), and C(1s) spectra with respect to the total N(1s) peak. The decrease in the atomic ratio of peak $1_{C(1s)}$ (Si–C) to the total N(1s) peak is in agreement with the formation of an Si_xN_y layer over the SiC-based Nicalon fibers.

The decreases observed in the peak $1_{O(1s)}$/total N(1s) and peak $2_{O(1s)}$/total N(1s) atomic ratios are primarily due to the removal of surface oxygen species accompanied by an increase in amounts of nitride and oxynitride formed.

A survey of the surface morphology of the nitrogen plasma treated fibers at 6000 times magnification revealed that the fibers exhibit a smooth Si_xN_y sheath and the absence of flaws and pitting. Thus, the surface treatment did not cause degradation of the fiber surface. This explains the retention of the tensile strength of the fibers even after surface treatment. The surface of the fiber was not degraded even after a 50-W nitrogen plasma treatment. The AES depth profile together with the scanning electron micrographs suggest that the Si_xN_y sheath formed around the fiber grows uniformly in thickness at high microwave power (>40 W).

Conclusions

Microwave nitrogen plasma treatment has been used to effectively modify the surface of Nicalon fiber. At low microwave powers, the surface carbonaceous layer is removed with the formation of silicon nitride and oxynitride. Various functional groups were also introduced in small amounts by surface treatment. These surface groups include –C–OH, –C–O–C–, C=O, and –C–N functionalities. At higher microwave powers (≥40 W), the amount of surface Si_xN_y is increased substantially while amounts of the other surface nitrogen functional groups remain low. High microwave powers result in the complete reduction of the surface SiO_2 layer with the active N species as well as an increase in the nitrogen penetration depth into the fiber. Silicon nitride formation is favored over silicon oxynitride. The treatment affects only the surface chemistry, leaving the bulk structure unchanged.

The results of the present study suggest the potential use of microwave nitrogen plasma pretreatment to form a thin Si_xN_y surface layer without degradation of the tensile strength and surface morphology. This layer may be used as a barrier layer for further fiber processing of fiber coatings.

Acknowledgment. This work was supported by the State of Connecticut, Department of Higher Education, High Technology Grant Number 42.

Registry No. SiC, 409-21-2; N, 7727-37-9.

Synthesis and Characterization of Poly[4-((*tert*-butoxycarbonyl)oxy)styrene–sulfone]

R. S. Kanga, J. M. Kometani, E. Reichmanis,* J. E. Hanson, O. Nalamasu,
L. F. Thompson, S. A. Heffner,* W. W. Tai, and P. Trevor

AT&T Bell Laboratories, 600 Mountain Avenue, Murray Hill, New Jersey 07974

Received January 17, 1991. Revised Manuscript Received April 1, 1991

Poly[4-((*tert*-butoxycarbonyl)oxy)styrene–sulfone] (TBSS) was synthesized by a thermally induced radical copolymerization of 4-((*tert*-butoxycarbonyl)oxy)styrene and sulfur dioxide using AIBN as the initiator. The effect of polymerization conditions such as temperature, monomer feed ratio, and monomer concentration on the copolymer molecular weight and composition was studied. The styrene–sulfone monomer sequence distribution was determined by NMR techniques, and the materials were found to be random copolymers of 4-((*tert*-butoxycarbonyl)oxy)styrene and SO_2. The monomer triad sequence distribution was identical for copolymers of equivalent composition prepared by different synthetic routes. The onset temperature for the thermal deprotection reaction decreases somewhat with increased incorporation of SO_2 relative to the parent styrene polymer, while the T_g increases. For imaging applications, it was determined that the extent of *tert*-butoxycarbonyl removal at a given dose decreased with increasing SO_2 content; a phenomenon that was ascribed to differences in the catalytic chain length and diffusion distance of the photogenerated acid.

Introduction

The *tert*-butyl protecting group[1] has been used extensively for the synthesis of polymers with acid or phenol functionalities that might otherwise be elusive. More recently, such chemistry has allowed the development of systems in which the ester group is removed by a thermally driven, catalytic reaction that is initiated by a photogenerated acid.[2-4] One application of such chemistry is in the area of microlithography. Specifically, polymers such as poly((*tert*-butoxycarbonyl)oxy)styrene)[2,3] have been used

---

(1) Green, T. W. *Protective Groups in Organic Synthesis*; Wiley: New York, 1981.

(2) Willson, C. G.; Ito, H.; Frechet, J. M. J.; Tessier, T. G.; Houlihan, F. M. *J. Electrochem. Soc.* **1986**, *133*, 181.

(3) Ito, H.; Willson, C. G.; Frechet, J. M. J. U.S. Patent 4,491,628, 1985.

(4) Houlihan, F. M.; Shugard, A.; Gooden, R.; Reichmanis, E. *Macromolecules* **1988**, *21*, 2001.

0897-4756/91/2803-0660$02.50/0

Scheme I

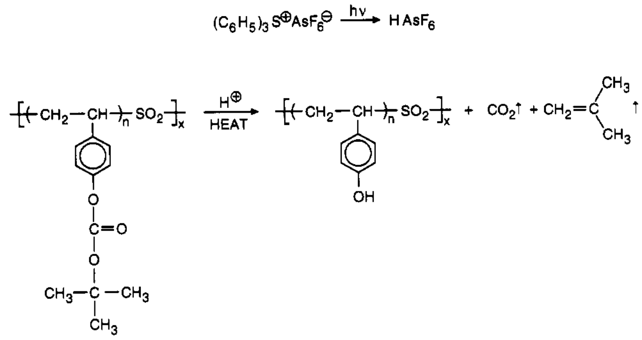

as matrix resins for chemically amplified resist formulations. In this scheme, a photogenerator of acid such as an onium salt[5] or nitrobenzyl ester[4] is added to the matrix polymer. Imagewise exposure liberates an acid within the polymer matrix in discrete areas, and subsequent mild heating liberates isobutylene and CO_2 to afford the hydroxystyrene resin. These steps effect a change in solubility of the matrix from an aqueous alkali-insoluble to alkali-soluble state, allowing pattern definition. Other materials issues such as the desirability of higher T_g (glass transition temperature) matrix polymers and polymers that would demonstrate improved radiation sensitivity when used in conjunction with nonionic acid generators such as the dinitrobenzyl esters led to the development of poly[4-((*tert*-butoxycarbonyl)oxy)styrene–sulfone] (TBSS).[6] The chemistry associated with the process outlined above utilizing TBSS is shown in Scheme I.

The synthesis of TBSS involves a thermally induced free-radical copolymerization of ((*tert*-butoxycarbonyl)-oxy)styrene (TBS) and sulfur dioxide (SO_2) using 2,2′-azobis(isobutyronitrile) (AIBN) as the initiator. Here, the effect of polymerization conditions such as reaction temperature and monomer concentration on polymer composition and molecular weight is evaluated, and the affect of incorporation of SO_2 into the polymer on the thermal characteristics of the system is examined. Additionally, the polymer molecular structure was determined by NMR analysis. Finally, an evaluation of the effects of copolymer composition on the efficiency of the deprotection reaction is presented.

Experimental Section

Materials Synthesis. Poly[4-((*tert*-butoxycarbonyl)-oxy)styrene–sulfone] (TBSS) was synthesized by a radical copolymerization of 4-((*tert*-butoxycarbonyl)oxy)styrene (TBS) and sulfur dioxide (SO_2) using 2,2′-azobis(isobutyronitrile) (AIBN) as the thermal initiator. The polymerization was carried out both in bulk and also with diluents such as liquid SO_2, dichloromethane, or toluene.

The monomer, TBS (Kodak), was purified by vacuum distillation (90 °C, 0.05 Torr) into several graduated ampules equipped with Rotaflo stopcocks. This arrangement allowed storage of the monomer under vacuum and addition of the monomer to the reaction vessel in vacuo without exposure to air.

Bulk polymerization was carried out in a thick-walled Kjeldahl flask suitably modified with stopcocks allowing for the addition of monomer in vacuo and distillation of SO_2 on the vacuum line. A known amount of AIBN (Aldrich, recrystallized from ethanol) was weighed into the reactor, which was then attached to the vacuum line and evacuated. An ampule containing TBS was attached to the reactor, and the monomer was then added to the flask through the stopcock. The reactor was cooled using liquid nitrogen, and anhydrous SO_2 (Matheson) was passed through a column of phosphorus pentoxide, condensed through the vacuum line into a graduated flask, and then distilled into the reactor. After removal of the reactor from the vacuum line, it was immersed into a constant-temperature bath, and the polymerization was allowed to proceed. The reaction mixture became viscous with time due to an increase in the polymer concentration and depletion of the monomer. The polymerization was terminated when the solution viscosity impeded stirring. The reaction was quenched by rapid cooling to ~0 °C (ice water) and careful opening of the stopcock to atmospheric pressure. The reaction mixture was diluted with acetone, and the polymer precipitated into methanol. The flaky white copolymer was further purified by redissolution into acetone followed by precipitation into methanol and drying in a vacuum oven overnight. This precipitation procedure was then repeated.

Solution polymerization was carried out using liquid SO_2, dichloromethane, or toluene as the diluent. The solvent (except liquid SO_2) was transferred into the reactor via a syringe under a constant flow of dry nitrogen, prior to attachment of the flask to the vacuum line. Subsequent manipulations were the same as for the bulk polymerization. When liquid SO_2 was used as the solvent, a predetermined volume of SO_2 was distilled into a graduated cylinder cooled in a dry ice/acetone bath before transferring into the reactor through the vacuum line. The reaction times were, in general, longer for solution polymerization. After a specific period, the contents of the reaction mixture were cooled to ~0 °C (ice water) and precipitated into excess methanol. Subsequent workup proceeded as described previously.

Poly(4-hydroxystyrene–sulfone) was prepared from TBSS in the following manner. To a solution of TBSS (5 g) in tetrahydrofuran (THF, 20 mL) was added trifluoromethanesulfonic acid (10 μL) under argon. The reaction mixture was stirred at room temperature under argon for 15 h. Precipitation from dichloromethane afforded the crude product, which was further purified by dissolution into THF and precipitation from dichloromethane. Vacuum filtration followed by drying at room temperature at reduced pressure afforded poly(4-hydroxystyrene–sulfone) (1 g) as a white powder.

Triphenylsulfonium hexafluoroarsenate was prepared as described in the literature.[7]

Polymer Characterization. Size exclusion chromatography (SEC) was used for determination of the molecular weight (MW) and molecular weight distribution (MWD) of TBSS. The eluting solvent was tetrahydrofuran (THF) at 35 °C (flow rate 1 mL/min). A Waters Model 510 pump (column pressure 900 psi) was used in conjunction with a Waters Model 410 differential refractometer detector and a Viscotek Model 100 differential viscometer detector. A series of 2 Polymer Laboratories mixed-bed (5–10 μm) PLgel columns was employed. A universal calibration curve was obtained by using narrow-MWD linear polystyrene standards supplied by the Toya Soda Co. Data acquisition and analysis were performed by an AT&T 6312 microcomputer equipped with a 12-bit A/D card and an ASYST Unical 3.02 software system supplied with the Viscotek detector.

Thermogravimetric analysis (TGA) and differential scanning calorimetry (DSC) data were obtained by using a Perkin-Elmer-TGS-7 thermogravimetric analyzer and DSC-4 differential scanning calorimeter, respectively, that were interfaced with a System 4 microprocessor and a TADS Model 8700 data station. Samples were heated from 20 to 450 °C at a heating rate of 10 °C/min. Samples ranged in mass between 1.20 and 2.00 mg. All measurements were obtained in ultrahigh-purity N_2 with a gas flow rate of 20 cm^3/min.

The copolymer composition was determined by elemental analysis (Galbraith Laboratories, Knoxville, TN) and calculation of the fraction of the repeat unit from the sulfur concentration. The sulfur concentrations were additionally determined via X-ray fluorescence, using the sulfur Kα X-ray line (2.308 keV). The X-ray fluorescence measurements were made in a Bell Laboratories X-ray milliprobe spectrometer. The X-ray milliprobe consists of a Varian Cr-target X-ray tube and enclosed sample chamber with a 1-mm-diameter sampling region, a Princeton Gamma-Tech lithium-drift silicon energy dispersive detector, and

---

[5] Crivello, J. V. *Polym. Sci. Technol.* **1984**, *29*, 351.

[6] Tarascon, R. G.; Reichmanis, E.; Houlihan, F. M.; Shugard, A.; Thompson, L. F. *Polym. Eng. Sci.* **1989**, *29*, 850.

[7] Crivello, J. V.; Lam, J. H. W. *J. Polym. Sci., Polym. Chem. Ed.* **1979**, *317*, 977.

Table I. Bulk Copolymerization of 4-((*tert*-Butoxycarbonyl)oxy)styrene and Sulfur Dioxide

run	temp, °C	time, h	moles of TBS added	conversion of TBS,[a] %	monomer feed ratio [TBS]:[SO_2]	copolymer composition[b] [TBS]:[SO_2]	moles of TBS/moles of AIBN	$10^5\bar{M}_w$	MWD ($\bar{M}_w/\bar{M}_n$)
1	65	2.0	0.4545	63.5	1:2.8	2.5:1	33	1.03	1.53
2	65	1.3	0.4545	70.6	1:2.3	2.8:1	33	1.21	1.69
3	65	1.0	0.4545	62.6	1:1.7	3.7:1	50	1.82	1.98
4	65	2.0	0.4545	56.5	1:2.8	2.6:1	50	1.53	1.60
5	66	2.1	0.4410	64.9	1:2.9	2.6:1	32	1.00	1.56
6	68	2.3	0.4545	74.7	1:2.8	2.6:1	33	0.93	1.54

[a] Conversion of TBS = final yield of copolymer (grams) × fraction of TBS incorporated/grams of TBS added. [b] From X-ray fluorescence.

Table II. Solution Copolymerization of 4-((*tert*-Butoxycarbonyl)oxy)styrene and SO_2

run	temp, °C	time, h	solvent, mL	moles of TBS added	conversion of TBS,[a] %	monomer feed ratio [TBS]:[SO_2]	copolym composition [TBS]:[SO_2]	moles of TBS/moles AIBN	$10^5\bar{M}_w$	MWD $\bar{M}_w/\bar{M}_n$
1a	40	40	liquid SO_2, 19[c]	0.099	37.3	1:4.9	1.9:1	100	5.3	1.9
1b	40	40	liquid SO_2, 27[c]	0.107	36.6	1:6.5	1.9:1	103	4.7	1.9
2a	60	6.5	liquid SO_2, 17[c]	0.086	38.7	1:5.1	2.1:1	102	1.7	1.7
2b	60	6.5	liquid SO_2, 25[c]	0.099	26.1	1:6.5	2.2:1	102	1.6	1.6
3	60	6.5	CH_2Cl_2, 17	0.102	36.8	1:1.1	3.0:1	100	1.6	1.6
4	60	6.5	CH_2Cl_2, 15.0	0.102	36.1	1:2.0	2.5:1	100	1.6	1.6
5	60	6.5	toluene, 15.5	0.097	35.9	1:1.0	3.8:1	100	1.7	1.6
6	60	6.5	toluene, 15.0	0.102	37.3	1:2.0	2.8:1	100	1.7	1.6

[a] Conversion of TBS = final yield of copolymer (grams) × fraction of TBS incorporated/grams of TBS added. [b] From C, H, O, S analysis (Galbraith). [c] Volume (mL) of SO_2 measured at −78 °C.

a Princeton Gamma-Tech System 4 analyzer. All the samples, both standards and unknowns, were carefully weighed and pressed into uniform pellets of approximately 1-mm thickness. Prior to each set of analyses, samples of known sulfur concentration (determined by wet chemical techniques) spanning the concentration range of interest were measured by X-ray fluorescence, and a linear calibration curve was established. The unknown samples were subsequently measured, and the sulfur concentrations were determined from the calibration curve. Two measurements were made on each sample to ensure reproducibility. The sample chamber was thoroughly flushed with helium both before and during the X-ray fluorescence measurements so as to eliminate any degradation of the sample due to X-ray-induced ozone production from residual oxygen in the sampling region. In addition, several samples were exposed to the X-ray beam for long times under these conditions to verify that there was no deterioration of the sample during the course of the X-ray fluorescence measurements. Under these conditions, sulfur concentrations were determined with a relative accuracy of 5%.

^{13}C and ^1H NMR spectra were recorded at 50 °C on a JEOL GX-500 spectrometer at resonance frequencies of 125 MHz for carbon and 500 MHz for proton. The 20–30 wt % samples were prepared in chloroform-*d* for the TBSS copolymers and *p*-dioxane-d_8 for poly(4-hydroxystyrene) and poly(4-hydroxystyrene–sulfone). The quantitative carbon spectra were collected with gated decoupling without the nuclear Overhauser effect and a pulse delay of 15s.

Deprotection Efficiency. Solutions were prepared by dissolving the matrix polymer in cyclohexanone (15 w/v %) followed by addition of triphenylsulfonium hexafluoroarsenate (2.7 mol % with respect to the moles of (*tert*-butoxycarbonyl)oxy groups in the polymer). The solutions were then filtered through a series of 1.0-, 0.5-, and 0.2-μm Teflon membrane filters, spin-coated onto oxidized silicon substrates, and baked at 105 °C for 2 min. The polymer–onium salt coated substrates were then exposed by using a GCA laserstep prototype deep-UV exposure tool operating at 248 nm. After exposure, the substrates were postexposure-baked at 115 °C for 20 s on a hot plate equipped with a vacuum hold-down chuck. The exposed and baked films were then developed in 0.17 N tetramethylammonium hydroxide for 45 s. Sensitivity was taken to be the minimum irradiation dose required to completely remove the film in the exposed regions with no loss of film thickness in the unexposed portions of the film. Resolution and image quality were determined by examining developed patterns with a JEOL Model 35CFS scanning electron microscope (SEM).

The extent of *tert*-butoxycarbonyl (*t*-BOC) removal was determined by FT-IR spectroscopy using a Mattson Instruments Inc. Galaxy Series Model 8020 spectrometer.

Results and Discussion

Polymer Synthesis. In this investigation, the thermal free-radical polymerization of TBS and SO_2 was carried out using AIBN as the initiator. Selective results from the bulk copolymerization are summarized in Table I, and those from the solution copolymerization are given in Table II. For the purposes of this discussion, the term bulk polymerization is used to define those reactions where the styrene monomer constitutes the major volume fraction of material. Thus, when the volume of SO_2 (or other solvent) is greater than that of TBS, the polymerization is considered to be a solution polymerization. The bulk copolymerizations had, in general, shorter reaction times and higher conversions than those carried out in solution. While the higher initiator concentration employed in the bulk reactions contributes to this observation, it is unlikely that decreasing the amount of initiator to the level used in the solution reactions would effect as significant a reduction in rate and conversion as was observed. Note that changing the TBS/AIBN ratio from 33 to 50 shows little effect on the conversion (run 1 vs 4, Table I). It should be noted that the initiator concentration generally was chosen so as to provide polymers with MWs in the range 100 000–250 000.

Polymer Characterization. The copolymer compositions were determined from the sulfur concentrations obtained from X-ray fluorescence analysis. These results were consistent with those obtained from elemental analysis.

Both proton and carbon NMR spectra were recorded for selected TBSS copolymers. Overlap of the methine and methylene proton resonances limits the usefulness of the copolymer proton spectra without selective deuteration of the styrene monomer.[8,9] However, the carbon spectra do allow a detailed examination of the monomer sequence distributions for the copolymers. The aliphatic region of

---

(8) Iino, M.; Katagiri, K.; Matsuda, M. *Macromolecules* **1974**, *7*, 439.
(9) Bae, H.; Miyashita, T.; Iino, M.; Matsuda, M. *Macromolecules* **1988**, *21*, 26.

Table III. Monomer Triad Sequences of Select Poly[4-((*tert*-butoxycarbonyl)oxy)styrene–sulfone] Determined by ^{13}C NMR Analysis[a]

sample	solvt	temp, °C	feed ratio TBS:SO$_2$	MSM	SMM	MMS	MMM	R^b TBS/SO$_2$	copolym[c] composition TBS:SO$_2$	4-hydroxy-styrene sequences, %
1	bulk	55	1:2.2	0.299	0.315	0.299	0.086	2.17	1.94:1	<1
2	bulk	65	1:2.2	0.276	0.258	0.276	0.191	2.88	2.70:1	NO[d]
3	bulk	65	1:1.7	0.095	0.115	0.095	0.694	7.70	8.1:1	2
4	liquid SO$_2$	60	1:6.5	0.296	0.319	0.296	0.085	2.13	2.10:1	3
5	CH$_2$Cl$_2$	60	1:1.1	0.244	0.237	0.244	0.276	3.21	3.00:1	2
6	toluene	60	1:1.0	0.192	0.205	0.192	0.410	3.88	3.80:1	NO[d]

[a] M = TBS; S = SO$_2$. No SMS detected. [b] $R = P(\mathrm{M})/1 - P(\mathrm{M})$; $P(\mathrm{M}) = p(\mathrm{MMM}) + p(\mathrm{MMS}) + p(\mathrm{MSM})$; $1 = p(\mathrm{SMS}) + p(\mathrm{MSM}) + p(\mathrm{SMM}) + p(\mathrm{MMS}) + p(\mathrm{MMM})$. [c] From C, H, O, S analysis (Galbraith). [d] Not observed.

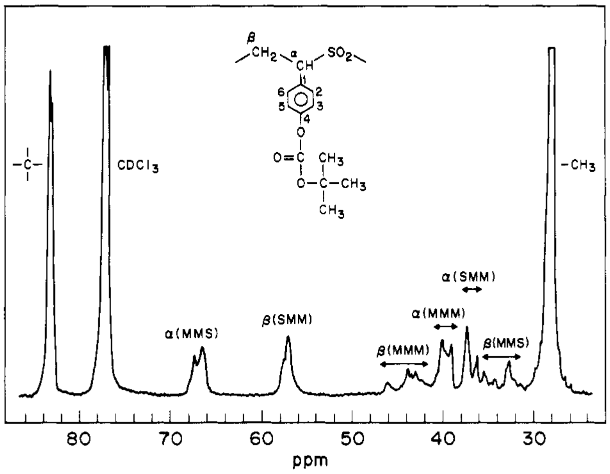

Figure 1. Aliphatic region of the ^{13}C NMR spectrum of sample 5, Table III. Solvent CDCl$_3$, 50 °C.

the carbon-13 NMR spectrum for a TBSS copolymer is shown in Figure 1. The chemical shifts of the α- and β-backbone resonances are not affected by the substitution of the (*tert*-butoxycarbonyl)oxy group on the styrene ring in the TBSS copolymers. The monomer triad sequence assignments were made by comparison with those published previously for poly(styrene–sulfone).[10] As reported by Cais et al.,[10] under these polymerization conditions MSM triads are not present in the samples. Further analysis of the multiple methine resonances enabled Cais et al.[10] and Bae et al.[9] to make tetrad sequence assignments to this stereoinsensitive carbon by observing changes in the relative intensities of these resonances as the sulfone content was varied. For example, the high-field component of the α(SMM) doublet is assigned to the α(SMMS) tetrad (36.48 ppm), and the low-field resonance is assigned to the α(SMMM) tetrad (37.64 ppm) since the intensity of α-(SMMS) decreases as the sulfone content is decreased. A combination of monomer sequences and stereosequence effects is responsible for the multiple resonances observed for the methylene carbons.[10] Bae et al. has assigned the upfield resonance of the β(MMS) triad to the β(SMMS) tetrad (32.42 ppm). Our data also support this assignment; however, the observation of multiple downfield resonances for the β(MMS) triad suggests that stereosequence effects contribute to the β(MMMS) tetrad. The unconditional probabilities of the five possible monomer triad sequences and the R values (TBS/SO$_2$) derived from the carbon spectra by using the equations in ref 3 are shown in Table III. The R values thus obtained were consistent with those derived from elemental analysis (Table III) and from X-ray fluorescence. Further details of the NMR characterization for these TBSS copolymers will be published elsewhere.

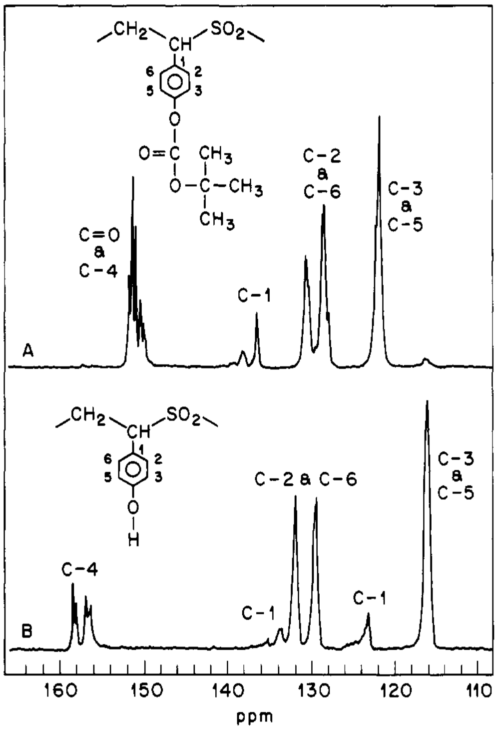

Figure 2. Aromatic region of the ^{13}C NMR spectra at 50 °C of (A) sample 4, Table III in CDCl$_3$ and (B) poly(4-hydroxy-styrene–sulfone) in *p*-dioxane-d_8.

Examination of the monomer triad sequences for samples 1 and 4 in Table III shows that the sequence distributions are equivalent upon either bulk or SO$_2$ solution polymerization for copolymers with similar R values. A similar comparison can be made between the sequence distributions of styrene–SO$_2$ copolymers obtained via bulk polymerization at 60 °C, $R = 3.03$ (ref 10, sample 4) and the TBS–SO$_2$ materials prepared in CH$_2$Cl$_2$ solutions (this work, sample 5, Table III) at 60 °C and a similar R value. We observe, as reported previously,[9] that the monomer sequence distributions depend only on the copolymer composition and not on the polymer source, i.e., bulk vs solution polymerization. Clearly, polymerization conditions determine the TBS-to-SO$_2$ ratio; however, two or more polymers of the same composition obtained under different reaction conditions have the same monomer sequence distribution.

Some discussion of the downfield aromatic region of the carbon-13 spectra of the TBSS copolymers is warranted. Parts A and B of Figure 2 show the aromatic region for a TBSS copolymer and poly(4-hydroxystyrene–sulfone), respectively. The quaternary C-1 carbons experience shielding effects from the polymer backbone SO$_2$ groups, causing two sets of resonances for these carbons. Attached

---

(10) Cais, R. E.; O'Donnell, J. H.; Bovey, F. A. *Macromolecules* **1977**, *10*, 254.

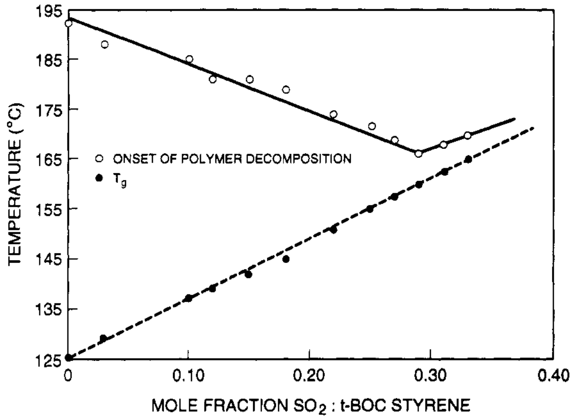

Figure 3. Plot of T_g (●) and onset of *t*-BOC removal (○) vs mole fraction of SO_2 in a series of TBSS copolymers.

proton test (APT) NMR experiments[11] of the protected polymer, distinguishing resonances by carbon types, assigns the quaternary C-1 carbons to the envelope of peaks between 136 and 139 ppm and the upfield resonances at 127.8 and 129.4 ppm. These upfield resonances increase in intensity with increasing SO_2 content and overlap with the broad C-2 and C-6 resonances at 128.6 and 130.6 ppm. The upfield C-1 resonances of the hydroxystyrene–sulfone polymer (Figure 2B) resonate between 123 and 126 ppm. Two sets of resonances are also observed for the C-2 and C-6 carbons. The downfield resonances decrease in intensity as the content of SO_2 groups is decreased. In this case, the carbons are deshielded by the backbone SO_2 groups. In both of the polymers a single broad resonance is observed for the aromatic 3 and 5 carbons (Figure 2). The multiplicity observed for the C-4 carbons is due to the monomer sequence distributions of the four tetrads (MMMM, SMMM, MMMS, and SMMS) possible with the polymerization conditions used. Stereosequence effects can be eliminated because this splitting is not observed in the spectrum of poly(4-hydroxystyrene). The carbonyl carbon of the *t*-BOC polymer also resonates in the region with the C-4 carbons.

Deprotection by the loss of the *tert*-butoxycarbonyl (*t*-BOC) group and the formation of poly(4-hydroxystyrene–sulfone) prior to irradiation would be expected to alter the lithographic performance of the TBSS copolymer. The extent of this deprotection can be monitored in the aromatic region of the carbon-13 NMR spectra. Comparison with poly(4-hydroxystyrene–sulfone) identifies the broad resonance (116 ppm) found in most of the copolymers as the C-3 and C-5 ring carbons of the deprotected polymer (Figure 2). The integrated amounts of the deprotected polymer found in each TBSS copolymer are summarized in Table III. Additional studies are needed to determine the origin of the deprotection reaction.

The thermal characteristics of select TBSS copolymers are shown in Figure 3. When plotted as a function of the mole fraction of SO_2 in the polymer, the glass transition temperature (T_g) of the material is seen to increase with increasing SO_2 content. For instance, the ((*tert*-butoxycarbonyl)oxy)styrene homopolymer exhibits a T_g of only 125 °C, whereas a TBSS copolymer having a TBS:SO_2 ratio of 2.5:1 (0.29 mol % SO_2) has a T_g that is 35 °C higher, namely, 160 °C. The observed increase in T_g can lead to significant processing advantages in situations where thermal flow must be minimized. One example is in imaging applications where image integrity must be maintained at elevated temperatures. In comparison to poly[((*tert*-butoxycarbonyl)oxy)styrene], the thermally driven reaction leading to loss of the *t*-BOC group in TBSS occurs at a somewhat lower temperature. For example, a polymer having a TBS:SO_2 ratio of 3:1 (0.25 mol % SO_2) exhibits loss of *t*-BOC beginning at 172 °C, a temperature 20 °C lower than that observed for the parent homopolymer. The decrease in the onset temperature is linear and inversely proportional to the SO_2 content up to a mole fraction of SO_2 of 0.29 (TBS:SO_2 of 2.5:1). After this point, the onset temperature is seen to increase with increasing SO_2 content. The hydroxystyrene–sulfone resins that are generated upon thermolysis of TBSS are stable to a temperature of ~250 °C.

Table IV. Effect of Feed Ratio, Temperature, and Solvent on Copolymer Composition

feed ratio TBS:SO_2	temp, °C	solvt	copolym composition TBS:SO_2
1:1	40		2.0:1
	60		2.5:1
	60	CH_2Cl_2	3.0:1
	60	toluene	3.8:1
1:2	60	CH_2Cl_2	2.5:1
	60	toluene	2.8:1
1:5	40	SO_2	1.9:1
	60	SO_2	2.1:1
1:6.5	40	SO_2	1.9:1
	60	SO_2	2.1:1

Table V. Effect of Solvent on the Copolymer Composition

copolym feed TBS:SO_2	solvt[a]	vol monom:vol solvt	copolym composition TBS:SO_2
1:1	bulk		2.5:1
1:5.1	liquid SO_2	1.1:1.0[b]	2.1:1
1:6.5	liquid SO_2	0.86:1.0[b]	2.2:1
1:1	methylene chloride	1.3:1.0	3.0:1
1:2	methylene chloride	1.4:1.0	2.5:1
1:1	toluene	1.4:1.0	3.8:1
1:2	toluene	1.4:1.0	2.8:1

[a] Temperature of polymerization = 60 °C. [b] Volume of SO_2 measured at -78 °C.

Copolymerization Mechanism. The temperature of the polymerization reaction plays a pivotal role in determining polymer MW and composition. As expected, for similar reaction times conversion is higher at higher temperatures. The molecular weight was found to be inversely proportional to the temperature. Solution polymerization, using liquid SO_2 as the solvent, effects approximately a 3-fold decrease in molecular weight when the temperature is increased from 40 to 60 °C (Table II, runs 1a and 2a). These results are consistent with the fact that the kinetic chain length is inversely proportional to the radical concentration. The copolymer composition is also affected by a change in temperature; higher temperatures result in a modestly lower incorporation of SO_2 into the copolymer (Tables II and IV). It should be noted that a minimum of two polymerizations were run under each set of conditions to confirm the results. The molecular weight was determined with a precision of ±5%, and the copolymer composition could be determined within ±2.5% by using X-ray fluorescence.

Table V summarizes the effect of feed ratio, temperature, and solvent on copolymer composition. At low temperatures (40 °C), the copolymer composition was essentially independent of feed ratio, varying from 1.9:1 to 2.0:1 for the 1:6.5 and 1:1 TBS:SO_2 ratios, respectively. At higher temperatures, the monomer feed ratio plays a more significant role. Note that at 60 °C a copolymer having a TBS:SO_2 ratio of 2.1:1 was obtained for both reactions

---

(11) Patt, S. L.; Shoolery, J. N. *J. Magn. Reson.* **1982**, *46*, 535–539.

where the TBS:SO_2 ratio was less than 1:5; however, a feed ratio of 1:1 yielded a 2.5:1 copolymer. When dichloromethane and toluene were used as the diluents, effectively decreasing the total monomer concentration (TBS plus SO_2), the extent of incorporation of TBS increased.

In comparing bulk vs solution polymerization (Tables I and II) it was seen that, in general, the rate and conversion increase with monomer concentration. This is expected since the rate of polymerization is directly proportional to the monomer concentration. Additionally, higher monomer concentration leads to higher molecular weight (Table II, runs 1a and 1b, and runs 2a and 2b). This result is a direct consequence of the dependence of the monomer concentration on the kinetic chain length for polymerization. The copolymer composition is also affected to some extent by the monomer concentration. In going from bulk to solution copolymerization, it is seen that incorporation of SO_2 in the copolymer decreases with dilution of the reaction mixture with a nonreactive solvent when the feed ratio is kept the same (Table V). For instance, at a monomer feed ratio of 1:1 and a temperature of 60 °C, the copolymer composition changed from 2.5:1 (TBS:SO_2) to 3.0:1 when dichloromethane was used as the solvent. Under similar conditions, toluene afforded a copolymer with a composition of 3.8:1. The difference in performance between dichloromethane and toluene as polymerization solvents is currently under investigation. Alternatively, when SO_2 is used as the "solvent" the level of incorporation of SO_2 is seen to increase.

The mechanism of propagation of styrene and SO_2 has been studied by a number of groups.[10,12-17] Barb[12,13] claimed that the copolymer composition of poly(styrene-sulfone could be accounted for by the participation of a styrene–SO_2 charge-transfer (CT) complex, C, shown in eq 1.

$$\mathrm{St} + \mathrm{SO_2} \overset{K_c}{\rightleftharpoons} \mathrm{C} \qquad (1)$$

Existence of a CT complex between styrene and SO_2 has been confirmed spectrophotometrically,[16] with the intensity of the absorbance due to the complex reaching a maximum value when the volume percent of styrene is ~50%. This suggests the existence of an equimolar styrene–SO_2 complex.

Matsuda[15-17] questioned the participation of the CT complex in the reaction mechanism and suggested that the copolymer composition of the styrene–SO_2 system could be explained on the basis of a second-order depropagation reaction of the sulfonyl radical to afford a styryl radical ($St^\bullet$) and SO_2 at lower temperatures (eq 2). In addition, at ambient temperatures and above, a first-order depropagation (eq 3), is also observed. The second-order propagation reaction of SO_2 is shown in eq 4, and that of styrene in eqs 5 and 6.

$$\sim\mathrm{St{-}SO_2^\bullet} + \mathrm{St} \xrightarrow{k_{d2}} \mathrm{St{-}St^\bullet} + \mathrm{SO_2} \qquad (2)$$

$$\sim\mathrm{SO_2^\bullet} \xrightarrow{k_{d1}} \sim\mathrm{St^\bullet} + \mathrm{SO_2} \qquad (3)$$

$$\sim\mathrm{St^\bullet} + \mathrm{SO_2} \xrightarrow{k_{pMS}} \sim\mathrm{St{-}SO_2^\bullet} \qquad (4)$$

$$\sim\mathrm{SO_2^\bullet} + \mathrm{St} \xrightarrow{k_{pSM}} \sim\mathrm{SO_2{-}St^\bullet} \qquad (5)$$

$$-\mathrm{St^\bullet} + \mathrm{St} \xrightarrow{k_{pMM}} -\mathrm{St{-}St^\bullet} \qquad (6)$$

Cais et al.[10] felt that the presence of a concerted second-order depropagation reaction (eq 2) is unlikely. The existence of St–St sequences was more simply ascribed to a first-order depropagation (eq 3) followed by a propagation similar to that in eq 6.

The TBS/SO_2 copolymerization behaves similarly to the styrene/SO_2 system studied by Barb,[12,13] Matsuda,[15-17] and Cais.[10] Thus at ambient temperatures and above, it is reasonable to assume that k_{pMS}, $k_{d1} \gg k_{pSM}$, k_{d2}, k_{pMM}. Also, at these high temperatures, the homopropagation of TBS (eq 6) is essentially irreversible. This results in an increased incorporation of TBS with increasing temperatures (Tables II and IV).

The decreased incorporation of SO_2 upon dilution could be explained by considering that propagation is a second-order reaction (eqs 4–6), whereas depropagation (at high temperatures) is a first-order process (eq 3). Therefore, upon dilution, the second-order rate of propagation is decreased relative to the first-order of depropagation. This allows eq 3 to contribute more to the overall composition and directly results in decreased incorporation of SO_2 upon dilution.

The effect of using liquid SO_2 as the copolymerization solvent is worthy of comment. From the theory of the dilution effect,[9,10,12] a decrease in the incorporation of SO_2 is expected upon increased dilution. However, in this case, the solvent is also a polymerizable monomer, and the previous statement does not hold. If a CT complex is involved in the propagation reaction, an increase in the incorporation of SO_2 will be observed as a consequence of an increase in the concentration of the complex in liquid SO_2. As seen in Table IV, this is indeed the result observed. Note that changing the feed ratio of TBS:SO_2 from 1:1 to 1:5 effects a change in the copolymer composition from 2.5:1 to 2:1. This result may be used as evidence supporting the claim[11,12] that a charge-transfer complex could be involved in styrene–SO_2 polymerizations under certain conditions.

In summary, the TBS/SO_2 radical copolymerization is quite complex and affected by a variety of factors, with temperature playing a critical role. An increase in reaction temperature leads to a decrease in the MW and decreased incorporation of SO_2. The copolymer composition was also affected by the feed ratio at high temperatures (60 °C and above) and low values of the feed ratio. Decreasing the monomer concentration results in a decrease in molecular weight and decreased incorporation of SO_2 when dichloromethane and toluene are used as solvents. Increased incorporation of SO_2 was observed when liquid SO_2 was used as a solvent.

Polymer Deprotection and Imaging. The effect of incorporation of SO_2 into the TBS-based matrix polymer on polymer deprotection and imaging efficiency was evaluated primarily by IR spectroscopy. Experiments were carried out comparing the efficiency of the deprotection reaction in TBSS materials having a TBS:SO_2 ratio of 3:1, 4.5:1, and 9:1 using triphenylsulfonium hexafluoroarsenate as the photoacid generator. The concentration of the arsenate onium salt was initially maintained at 2.7 mol % relative to the number of moles of *t*-BOC groups in the respective polymers. Figure 4 compares the IR carbonyl stretch at 1756 cm^{-1} for TBSS/onium salt compositions before and after exposure to 248-nm radiation (4 mJ/cm^2) followed by postexposure bake to effect the acid-induced

---

(12) Barb, W. G. *Proc. R. Soc. London* **1952**, *A212*, 509.
(13) Barb, W. G. *J. Polym. Sci.* **1953**, *10*, 49.
(14) Walling, C. *J. Polym. Sci.* **1955**, *16*, 315.
(15) Matsuda, M.; Iino, M. *Macromolecules* **1969**, *2*, 216.
(16) Matsuda, M. *Prog. Polym. Sci., Jpn.* **1971**, *2*, 49.
(17) Matsuda, M.; Iino, M.; Hirayama, T.; Miyashita, T. *Macromolecules* **1972**, *5*, 240.

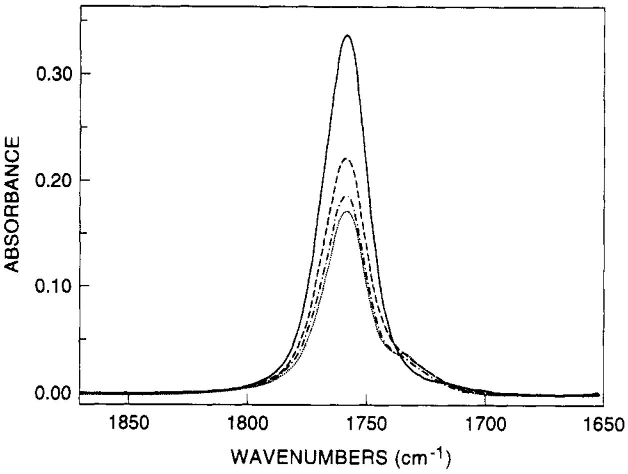

Figure 4. FT-IR spectra of the carbonyl stretch of TBSS before and after exposure to 248-nm radiation (4 mJ/cm^2) and postexposure bake; TBSS (3:1) before exposure (—), TBSS (3:1) after exposure and PEB (- -), TBSS (4.5:1) after exposure and PEB (-•-), TBSS (9:1) after exposure and PEB (•••).

Table VI. Extent of *t*-BOC Remaining for a Series of TBSS Copolymers Formulated with Triphenylsulfonium Hexafluoroarsenate

	rel % *t*-BOC remaining					
	3:1[a]		4.5:1[a]		9:1[a]	
dose, mJ/cm^2	2.7 mol % PAG[b]	5 wt % PAG	2.7 mol % PAG	5 wt % PAG	2.7 mol % PAG	5 wt % PAG
0	1.0	1.0	1.0	1.0	1.0	1.0
1	0.96	0.96	0.93	0.94	0.95	0.94
2.5	0.84	0.86	0.78	0.80	0.73	0.77
4	0.72	0.76	0.63	0.67	0.56	0.61
7	0.45	0.55	0.34	0.43	0.30	0.33
10	0.26	0.36	0.17	0.24	0.16	0.19
13	0.15	0.22	0.10	0.09	0.05	0.08
16	0.09	0.16	0.04	0.06	0.03	0.04
19	0.05					

[a] Values denote the ratio of TBS:SO$_2$ in the TBSS copolymers evaluated. [b] Triphenylsulfonium hexafluoroarsenate.

deprotection reaction. For clarity, only the absorbance for the 3:1 polymer is shown prior to exposure. The 4.5:1 and 9:1 materials exhibited essentially identical spectra. Clearly, the efficiency of the deprotection reaction, as determined by the intensity of the carbonyl stretch of the *t*-BOC group (1756 cm^{-1}), *decreases* with *increasing* SO$_2$ content. While these differences diminish somewhat upon incorporation of equivalent weight percentages of the acid generator, polymers having higher TBS:SO$_2$ ratios still exhibit lower deprotection rates. Table VI compares the results obtained for the three TBSS materials examined here upon incorporation of both 2.7 mol % and 5 wt % acid generator.

The decreased efficiency of the deprotection reaction upon increased incorporation of SO$_2$ is somewhat surprising in light of previous lithographic results showing that the incorporation of SO$_2$ into TBS-based resins had essentially no effect on the lithographic sensitivity of the system when onium salts were used as the photoacid generators.[6] Additionally, the lithographic performance of the current series of materials exhibits marginal differences in the exposure dose required to clear images (~15 mJ/cm^2 for large area exposures and 31–35 mJ/cm^2 for 0.5-μm features).[18] Factors affecting the polymer deprotection and imaging include the catalytic chain length (moles of *t*-BOC removed per mole of acid generated), extent of acid diffusion, extent of radiation-induced main-chain scission of the styrene–sulfone matrix resin, and polymer solubility. The extent of acid diffusion in poly(TBS) is on the order of 50 Å, or the radius of gyration of one polymer molecule.[19] Assuming the diffusion distance is similar for the TBSS resins examined here, the extent of *t*-BOC removal should be the same for equivalent weight percent loadings of onium salt, i.e., one acid molecule will occupy the same volume fraction of material. Since the extent of deprotection in the TBSS resins decreased with increasing SO$_2$ content for both equivalent mole and weight percent loadings of acid generator, it is conceivable that HAsF$_6$ is less mobile within the olefin–sulfone matrix and that the observed acid-loss mechanism for poly(TBS)[19] occurs more readily in the sulfone analogues. In fact, the catalytic chain length for *t*-BOC removal decreases by 20% in going from the 9:1 to 3:1 copolymer, again indicating decreased acid mobility and an enhanced acid-loss mechanism. Since the differential dose required to image TBSS through acid-catalyzed *t*-BOC removal (~15 mJ/cm^2) vs a main-chain scission mechanism (~1–2 J/cm^2)[20] is substantial, it is unlikely that a significant number of chain scission events occur upon 15 mJ/cm^2 exposure. The lack of discernible differences in observed lithographic sensitivity most probably lies in differences in the solubility characteristics of the resins, with the more polar SO$_2$-containing polymers being more readily soluble in aqueous base media at slightly higher *t*-BOC concentrations.

Table VII. Effect of Postexposure Bake Conditions on Resist Sensitivity

	resist sensitivity, mJ/cm^2	
postexposure bake temp,[a] °C	triphenylsulfonium hexafluoroarsenate[b]	dinitrobenzyl tosylate[c]
90	22	175
115	22	40
130	22	20

[a] The bake time was 30 s. [b] 5 wt % formulated in TBSS (3:1). [c] 8.4 mol % formulated in TBSS (3:1).

One advantage regarding the use of TBSS as a matrix polymer arises from its thermal characteristics described above. Notably, the higher T_g of the resin allows the use of higher postexposure baking temperatures to effect enhanced sensitivity without loss of image fidelity. This is particularly important when weaker acids than HAsF$_6$ are used for deprotection. Consistent with reports that strong acids produced from onium salts have a catalytic chain length of ~1000 and that once this level is reached, no additional deprotection takes place,[19] TBSS/triphenylsulfonium hexafluoroarsenate resist formulations exhibit no change in resist sensitivity upon postexposure baking in the range of 90–130 °C (Table VII). However, changes in resist sensitivity are observed when benzenesulfonic acids are used as the catalysts. As noted in Table VII, significant changes in resist performance vs postexposure bake temperature are observed when TBSS is formulated with a substituted nitrobenzyl sulfonate acid generator such as 2,6-dinitrobenzyl tosylate. These differences arise from the lower reactivity of the sulfonic acid and the observed increase in catalytic chain length with reaction time and temperature.[21] An additional advantage of the higher

---

(18) Kometani, J. M.; Nalamasu, O.; Reichmanis, E.; Kanga, R. S.; Thompson, L. F.; Heffner, S. A. *J. Vac. Sci. Technol. B* **1990**, *8*, 1428.

(19) McKean, D. R.; Schaedeli, U.; MacDonald, S. A. In *Polymers in Microlithography*; ACS Symposium Series No. 412; Reichmanis, E., MacDonald, S. A., Iwayanagi, T., Eds.; American Chemical Society: Washington, DC 1989; pp 27–38.

(20) Bowden, M. J.; Chandross, E. A. *J. Electrochem. Soc.* **1975**, *122*, 1370.

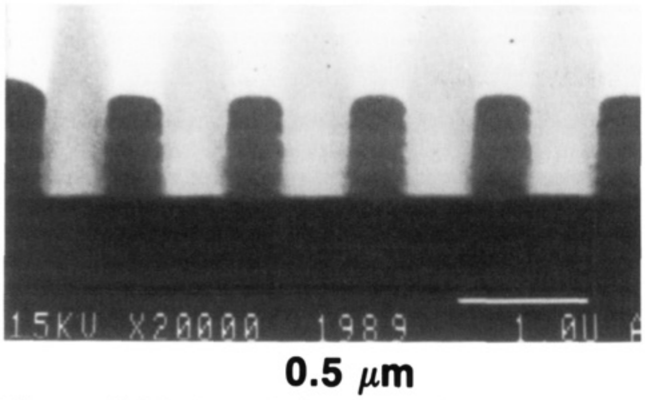

Figure 5. SEM micrograph depicting coded 0.5-μm images obtained in a 3:1 TBSS copolymer formulated with 5 wt % triphenylsulfonium hexafluoroarsenate.

T_g is that fully developed images may be treated at higher temperatures with no observed flow when TBSS is used as opposed to the parent styrene. The presence of up to 2% deprotection, as determined by NMR characterization, in TBSS did not affect the imaging characteristics of the system.

While some differences in resolution capability were observed for the materials described, it is not clear at this time whether the observed effects result from inherent materials characteristics or the lithographic process used to define the images. It does appear though, that sub-0.5-μm imaging is facilitated when the molecular weight of the copolymer is <300 000. A typical image that has been obtained in a TBSS resist system is depicted in Figure 5.

Summary

TBSS is readily prepared via thermally induced free-radical bulk or solution polymerization. The copolymerization conditions, e.g., temperature and monomer concentration, determine copolymer composition and molecular weight. The polymerization mechanism is complex but may be explained by the rate equations proposed by Barb, Matsuda, and Cais. ^{13}C NMR spectra of selected TBSS copolymers indicate that the monomer triad sequence distribution is identical for copolymers of equivalent composition prepared by different synthetic routes. ^{13}C NMR analysis was also useful in determining the extent of deprotection of the *t*-BOC moieties in the TBSS copolymers during copolymerization. The thermal deprotection reaction in TBSS occurs at approximately the same temperature as the parent styrene polymer, though the incorporation of SO_2 substantially raises the glass transition temperature. The extent of *t*-BOC removal at a given dose decreases with increasing SO_2 content in the polymer. This was ascribed to differences in the catalytic chain length and diffusion distance of the photogenerated acid. The imaging characteristics, however, remain unaffected, presumably due to solubility differences of the polymers.

Acknowledgment. We thank M. Cheng, D. A. Mixon, F. M. Houlihan, T. X. Neenan, F. C. Schilling, A. E. Novembre, G. N. Taylor, and L. E. Stillwagon for technical assistance and many useful discussions concerning various aspects of this work.

Registry No. TBS, 87188-51-0; TBSS (copolymer), 120332-58-3; SO_2, 7446-09-5.

---

(21) Houlihan, F. M.; Neenan, T. X.; Reichmanis, E.; Kometani, J. M.; Chin, T. *Chem. Mater.* **1991**, *3*, 462.

Synthesis and Characterization of a Catalytically Active Nickel–Silicoaluminophosphate Catalyst for the Conversion of Methanol to Ethene

J. M. Thomas,* Y. Xu, C. R. A. Catlow, and J. W. Couves

The Davy Faraday Research Laboratories, The Royal Institution, 21 Albemarle Street,
London, W1X 4BS UK

Received January 22, 1991. Revised Manuscript Received May 15, 1991

X-ray absorption (near-edge and extended fine structure) along with diffuse reflectance infrared spectroscopy and other techniques are used to characterize specially prepared crystalline powdered samples of the title catalyst, which is based on the chabazite framework. It is established that the nickel ions that are all in tetrahedral, framework sites (first shell Ni–O distance lying close to 1.98 Å), and the loosely bound extraframework protons are thought to be the key components of the catalyst for the highly selective conversion of methanol to ethene.

Introduction

There is a class of heterogeneous catalysts in which essentially all the atoms of the bulk of the solid participate directly or are implicated indirectly in the key catalytic processes of the overall reaction. Well-known examples are zeolites, the silicoaluminophosphates (SAPOs), metal–aluminophosphates (MeAPOs), and also the various ion-exchanged sheet aluminosilicate clays such as montmorillonite and their pillared variants.[1,2] In such solid catalysts the "active sites" are distributed in a more or less spatially uniform fashion throughout the bulk of the solid. This means that they are amenable to characterization by most of the traditional and recently developed techniques

---

(1) Thomas, J. M. *Angew. Chem., Int. Ed. Engl.* **1988**, *27*, 1673.
(2) Thomas, J. M. *Philos. Trans. R. Soc. London, A* **1990**, *333*, 173.

0897-4756/91/2803-0667$02.50/0